Submission code: ABV8M57ZBN

See this and other abstracts on our website: https://home.sbgf.org.br/Pages/resumos.php

Studying Anthropogenic Impacts on the Critical Zone: EACH-PET CZO Seed Site, São Paulo, Brazil

Leticia Rangel Dantas (IAG-USP), Andrea Ustra (Instituto de Astronomia; Geofísica e Ciências Atmosféricas da Universidade de São Paulo (IAG/USP)), Marina Fernandes Sanches Barros (UNESP), Rosely Aparecida Liguori Imbernon (EACH-USP), MARCELO STANGARI (UNIVERSIDADE DE SÃO PAULO (USP) - INSTITUTO DE ASTRONOMIA; GEOFISICA E CIENCIAS ATMOSFERICAS (IAG).)

Studying Anthropogenic Impacts on the Critical Zone: EACH-PET CZO Seed Site, São Paulo, Brazil

Abstract Summary

This study investigates the Critical Zone (CZ) in an urbanized floodplain. Critical Zone Observatories (CZOs) enable the monitoring of interactions among physical, chemical, and biological processes. Megacities, such as São Paulo, face socio-environmental issues resulting from intense urbanization. To address this, the EACH-PET CZO seed site is being implemented to understand the effects of anthropogenic impacts on the CZ. Architecture and subsurface fluid dynamics were assessed using electrical resistivity (dipole-dipole array) acquired during different periods. Soil magnetic mineralogy was characterized through χFD, SIRM, HIRM, and S-ratio. Resistivity contrasts highlight interfaces with variable grain sizes and water saturation, as well as potential methane migration. Variations in magnetic signatures suggest the influence of biogeochemical processes linked to water pollution and methanogenesis.

Introduction

The Critical Zone (CZ) is the region of the Earth's surface extending from vegetation to groundwater, involving complex interactions among physical, chemical, and biological processes (NRC, 2001; Anderson et al., 2007). Understanding how these processes evolve can aid the development of predictive models to responses to climate and land-use changes (Waldron, 2020). Critical Zone Observatories (CZOs) enable quantification of interaction mechanisms and identification of trends in the evolution of processes within the CZ (Brantley et al., 2017). Consequently, over the past 20 years, CZOs have been established in diverse geological, climatic, and land-use contexts (Zacharias et al., 2011; Banwart et al., 2013; Karan et al., 2016; Brantley et al., 2017; Gaillardet et al., 2018).

According to the UN-Habitat Annual Report 2022, by 2050, 68% of the global population will be urban, resulting in extensive modifications on the CZ. In anthropized areas, soil functions are often impacted by changes such as compaction and contamination. These modifications can affect soil structure, water flow, and redox dynamics, altering process rates and fluxes within the CZ (Minor et al., 2019). Therefore, the city of São Paulo was selected for establishing a seed site to study the Critical Zone as an example of physical environment degradation due to urbanization.

The EACH-PET OZC seed site involves collaboration among researchers from different fields at IAG-USP and EACH-USP. The studies have been conducted using an integrative and multidisciplinary approach, applying concepts and tools from geology, geophysics, geochemistry, and biology. The main objective of this work is to characterize the architecture and understand the seasonal dynamics of an urbanized floodplain influenced by natural (water level and vegetation cover) and anthropogenic (composition and backfill thickness) factors.

Methods

The study area is located in eastern São Paulo, southeastern Brazil (Figure 1). The OZC includes the School of Arts, Sciences and Humanities (USP East campus) and the Tietê Ecological Park, Engenheiro Goulart sector, within the Tietê River Floodplain Environmental Protection Area (APAVRT). APAVRT lies within the Upper Tietê Basin, a highly anthropized hydrological system due to intense urbanization, including soil sealing, backfilling floodplain, and river rectification and channelization (São Paulo, 2013).

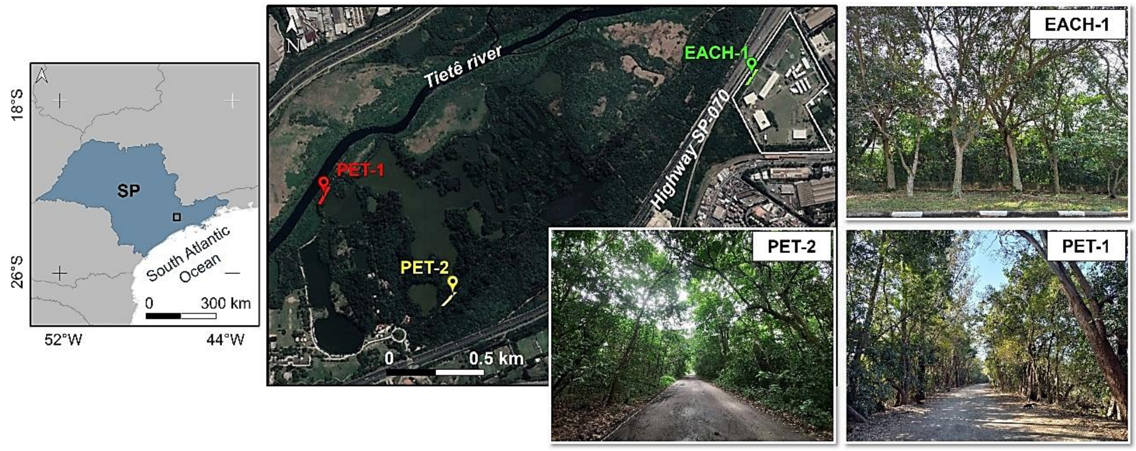

Figure 1: Location map of the study area. Lines indicate where geophysical acquisitions were performed, while markers show soil sampling locations.

Subsurface CZ architecture was characterized along three 110 m long profiles. Electrical resistivity (ER) data were acquired during both wet and dry seasons using 2D imaging with a dipole-dipole array. Measurements were performed with a SuperSting (AGI) system in automatic mode, using 56 electrodes. Acquisition planning and command file generation were done in SSAdmin (AGI). Electrode spacing ranged from 1.0 to 4.0 m to improve resolution in the vadose zone while maintaining sensitivity below the water table. Pseudosections were generated through data inversion using RES2DINV version 4.10.20 (Iris Instruments).

Soil samples were collected at 0.5 m intervals during the drilling of groundwater monitoring wells. Magnetic characterization was carried out at the Paleomagnetism and Rock Magnetism Laboratory (USPMag, IAG-USP). Magnetic susceptibility was measured at two frequencies (976 Hz and 15.616 Hz) using a Kappabridge MFK1-FA susceptometer (AGICO), at room temperature with a 200 A/m AC field. Isothermal remanent magnetization (IRM) was measured with a SQUID RAPID SYSTEM rock magnetometer (2G Enterprises) after applying magnetic fields of 1.0 T, –0.1 T, and –0.3 T using an MMPM10 pulse magnetizer (Magnetic Measurements Ltd.). These values were used to calculate SIRM, S-ratio, and HIRM.

Results

Pseudosections from the three profiles show a horizontal resistivity contrast at approximately 2.0 m depth (Figure 2). Resistivity values above 384 Ω·m occur in the vadose zone, while values below 51.7 Ω·m correspond to the saturated zone. In PET-1, an additional contrast at 5.0 m is attributed to a textural transition from gravelly sand to clay. In PET-2, this transition occurs above 8.0 m depth. EACH-1 exhibits greater heterogeneity, with lateral resistivity variations at depth. At this site, organic-rich clayey sediments dredged from the Tietê River bed were subsequently backfilled. Therefore, resistivity anomalies (85.3–141 Ω·m) below the water table may indicate sandy lenses or methane pockets generated by the degradation of organic matter. Seasonal variations show lower resistivity during the dry season, likely due to moisture retention by plant roots. Changes in the saturated zone may reflect hydrogeological dynamics (mainly in PET-1 and PET-2) or methane migration (EACH-1).

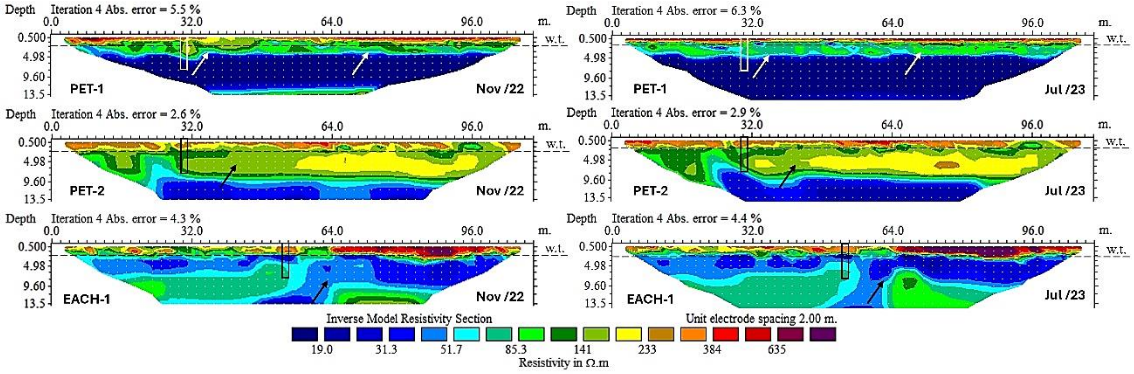

Figure 2: Electrical resistivity sections acquired during wet (Nov/22) and dry (Jul/23) periods. Polygons indicate monitoring well location in the line, while arrows show regions with seasonal variation. w.t. = water table.

Higher magnetic susceptibility values are observed in near-surface samples, typically linked to increased concentrations of nanometric ferrimagnetic minerals (e.g., magnetite, maghemite) from pedogenic processes. In EACH-1, however, these values may reflect redox variations due to changes in water saturation (~3.0 m) or microbial activity related to methanogenesis. χFD values >6% in the saturated zone of EACH-1 and PET-2 also indicate the presence of nanometric magnetite.

The S-ratio estimates the relative abundance of low- and high-coercivity minerals, such as magnetite (ferrimagnetic) and hematite (antiferromagnetic), respectively. Values above 0.5 indicate that more than 50% of the magnetization is retained by ferrimagnetic minerals. In contrast, the HIRM parameter reflects the concentration of antiferromagnetic minerals. Lower S-ratio and higher HIRM values suggest magnetic mineralogy indicative of oxidizing conditions. This pattern is most evident in PET-1, the profile closest to the river, where the magnetic signature at depth may reflect hydrogeological interactions between polluted surface waters (river and lake) and groundwater.

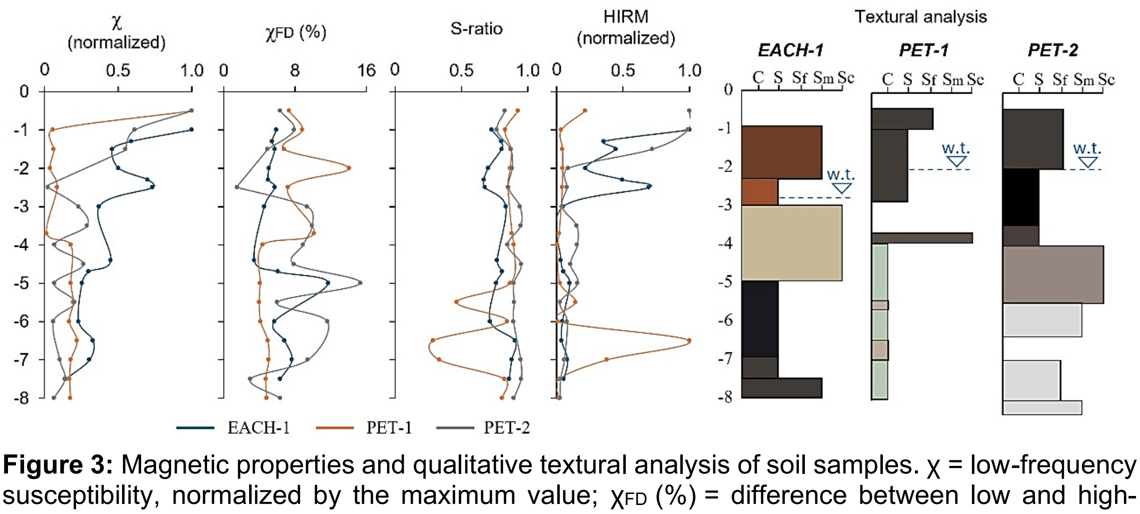

Figure 3: Magnetic properties and qualitative textural analysis of soil samples. χ = low-frequency susceptibility, normalized by the maximum value; χ_{FD} (%) = difference between low and high-frequency magnetic susceptibility; S-ratio = contribution of low-coercivity minerals; HIRM= isothermal remanent magnetization of high-coercivity minerals, normalized by the maximum value; C = clay; S = silt; Sf = fine sand; S_m = medium sand; S_C = fractions above coarse sand; w.t. = water table. The colors in the textural profile correspond to the colors of the material sampled during the monitoring wells installation.

Conclusions

In this work, we verify the influence of different hydrogeophysical and biogeochemical processes through variations in electrical properties and magnetic mineralogy, which reflect anthropogenic changes resulting from the urbanization process. The study presents evidence of the influence of interfaces with different granulometric contributions and water saturation on the variations in ferrimagnetic grain size and resistivity contrasts. The characterization of magnetic mineralogy (particle composition and size) also provided insights into biogeochemical processes dynamics involving changes in iron (hydr)oxides. Therefore, the EACH-PET OZC seed site can function as a natural laboratory to answer important questions about contaminant availability and evolution of environmental restoration processes.

Acknowledgments

The authors acknowledge the Coordenação de Aperfeiçoamento de Pessoal de Nível Superior (CAPES), the Fundação de Amparo à Pesquisa do Estado de São Paulo (FAPESP) process 2021/14808-6 and the Living Lab EACH Project.

References

Anderson, S. P., F. Von Blanckenburg, and A. F. White, 2007, Physical and Chemical Controls on the Critical Zone: Elements, 3, 315–319.

Banwart, S. A. J., J. Chorover, D. Gaillardet, D. T. Sparks, S. White, S. Anderson, et al., 2013, Sustaining Earth's critical zone: Basic science and interdisciplinary solutions for global challenges: Univ. of Sheffield, Sheffield, UK.

Brantley, S. L., W. H. Mcdowell, W. E. Dietrich, T. S. White, P. Kumar, et al., 2017, Designing a network of critical zone observatories to explore the living skin of the terrestrial Earth: Earth Surface Dynamics, 5, 841–860.

Bloemendal, J., J.W. King, F.R. Hall, and S.J. Doh, 1992, Rock magnetism of Late Neogene and Pleistocene deep-sea sediments: relationship to sediment source, diagenetic processes, and sediment lithology: J. Geophys. Res., 97, 4361-4375.

Gaillardet, J., I. Braud, F. Hankard, S. Anquetin, O. Bour, N. Dorfliger, et al., 2018, OZCAR: The French network of critical zone observatories: Vadose Zone Journal, 17.

Karan, M., M. Liddell, S. M. Prober, S. Arndt, J. Beringer, M. Boer, J. Cleverly, et al., 2016, The Australian SuperSite Network: A continental, long-term terrestrial ecosystem observatory: Science of the Total Environment, 568, 1263–1274.

Minor, J., J. K. Pearl, M. L. Barnes, T. R. Colella, P. C. Murphy, S. Mann, and G. A. Barron-Gafford, 2019, Critical Zone Science in the Anthropocene: Opportunities for biogeographic and ecological theory and praxis to drive earth science integration: Progress in Physical Geography.

National Research Council, 2001, Basic research opportunities in the earth sciences: Natl. Acad. Press, Washington, DC.

Robinson, S.G., 1986, The late Pleistocene palaeoclimatic record of North Atlantic deep-sea sediments revealed by magnetic mineral measurements: Phys. Earth Planet. In., 42, 22-47.

São Paulo, 2013, Plano de manejo Área de Proteção Ambiental da Várzea do Rio Tietê, volume principal, 711 p.

Waldron, P. Critical zone science comes of age. Eos, v. 101, 2020, doi: 10.1029/2020EO148734.

Zacharias, S., H. Bogena, L. Samaniego, M. Mauder, R. Fuß, T. Pütz, et al., 2011, A Network of Terrestrial Environmental Observatories in Germany: Vadose Zone Journal, 10, 955-973.